

Read-out using F1-TDC-ADC of the newSFD X plane (and dE/dx counter)

Fujio TAKEUTCHI

Sosuke HORIKAWA*

Faculty of Science, Kyoto Sangyo University, Kyoto, Japan

*Physik-Institut, Zurich University, Zurich, Switzerland

Abstract

The data of the SFD X-plane and dE/dx counter, obtained with a minimal DAQ were analyzed. Several features of the new F1-TDC-ADC device were checked. The optimal threshold settings for the future run are found to be 15 - 20 mV for X-plane, and 20 mV for dE/dx counter.

1. Introduction

The new X plane of Scifi hodoscope (newSFD) [1] was built and tested in 2006, and was mounted in the DIRAC[2] spectrometer in 2007. However, the preparation of the DAQ system was delayed, and for that reason, it was not possible to use it in the DIRAC data acquisition in 2007. Just before the shutdown, Sosuke Horikawa made a heroic effort to take some data, helped by Valery Brekhavsky, using a mini-DAQ program, which was developed only to read out a few 128 channels of F1-TDC-ADC. The trigger used in this data taking was mix2007.lst of the main DIRAC run, but no information on the rest of the DIRAC spectrometer is available in the obtained data. Two kinds of data were taken.

- 1) First 64 input channels were dedicated to the 4 planes of dE/dx counter, and only the first 64 channels out of 480 channels of X plane were read out.
- 2) All 128 channels were used to read out a part of the X plane. Four measurements were performed to scan all 480 channels of X plane.

The main objective of the measurement was to find the most appropriate hardware threshold for the read out of X plane, since it was already known that if the threshold is too low, not only the

multiplicity becomes too large but a lot of back ground actually reduces the detection efficiency, whereas if the threshold is too high, naturally we lose the efficiency. We intend to obtain an efficiency for singles which is higher than 98%, and a multiplicity not much higher than 1.05 after an off-line peak-sensing algorithm being applied. (1.05 is what we used to have with the PSC[3] circuit.)

As the information obtained with this reduced DAQ is so limited, it is very difficult to extract much information needed, but we try to extract as much information as we can get from the existing data.

In this short report, we call the new readout device “F1-TDC” or “F1-ADC”, but in reality, it is one device “F1-TDC-ADC” devised by V. Karpukhin. The detail of the device is explained elsewhere.

Fig. 1 shows a typical F1-ADC spectrum obtained from X plane obtained at threshold of 10 mV. The data reproduces fairly well the preliminary data we obtained in 2006[4] which is reproduced in Fig. 2.

One can observe in these two figures that the threshold is rather well reproducible. This is one of the advantages of this new device.

Fig. 3 shows a typical F1-TDC spectrum of all the events recorded in the trigger. The ADC spectrum shown in Fig. 1 includes all the events in the trigger.

2. ADC spectra of X plane

Fig. 4 shows the threshold dependence of the ADC spectra of X plane for the events included

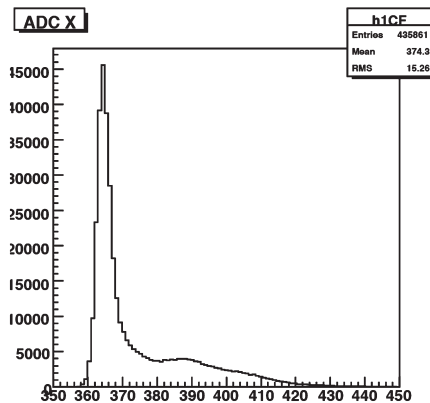


Fig. 1 A typical ADC spectrum obtained with F1-ADC for X plane. The threshold was at 10 mV. This contains all the events included in the trigger.

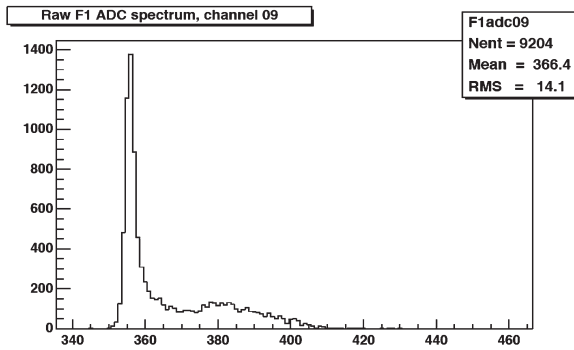


Fig. 2 ADC spectrum obtained with F1-ADC for the X plane in a test measurement at T11. The threshold was at 10 mV. The trigger was made with 3 beam counters before and after X plane.

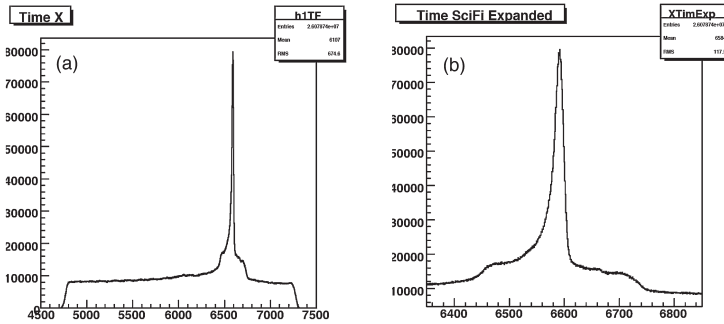


Fig. 3 TDC spectrum of X plane obtained using F1-TDC. The trigger used was mix2007.lst. The threshold was at 10 mV. The histogram on the right side (b) shows only the central part expanded.

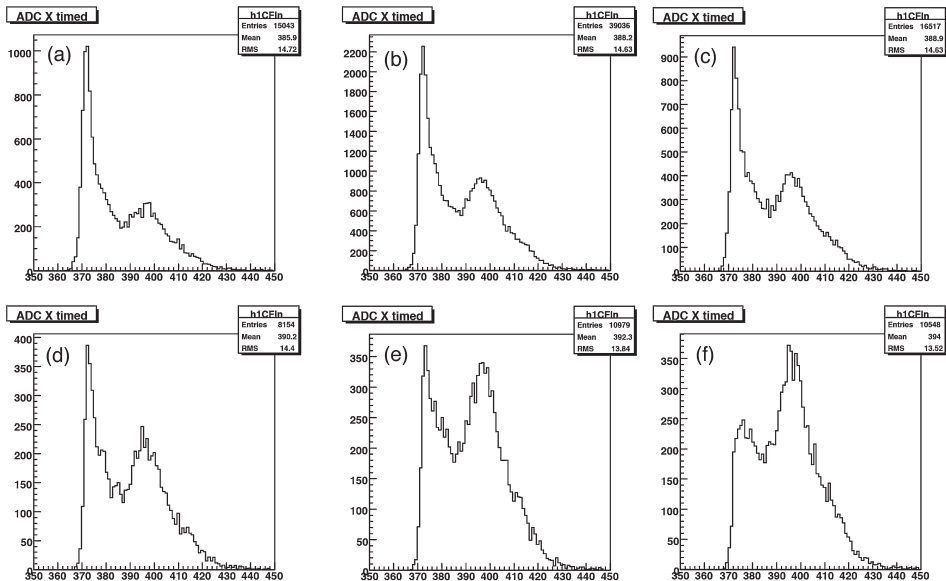


Fig. 4 ADC spectra obtained from X plane with F1-ADC at different thresholds. Events included are those contained in the narrow timing peak shown in Fig. 2 (coincident events). Figures are, for thresholds (a) 5 mV, (b) 10 mV, (c) 15 mV, (d) 20 mV, (e) 25 mV and (f) 30 mV.

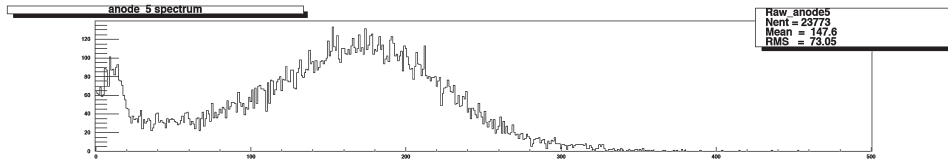


Fig. 5 For the sake of comparison, an ADC spectrum obtained using traditional ADC (LeCroy 2228A) is shown. The small peak on the left is due to the single photoelectrons. This peak is hardly visible in the spectra in Fig. 4 due to the broad “pedestal” peak

in the narrow peak in Fig. 3.

To compare the ADC spectrum obtained with F1-ADC with that obtained with traditional ADCs, we show in Fig. 5 an ADC spectrum obtained with LeCroy 2228A ADC in the past. In this spectrum, the pedestal which is at channel -1 with a width of 1 or 2 channels is not shown. The tiny peak seen at channel 15 is the single photoelectron peak. The ADC spectra shown in Fig. 4 obtained with F1-ADC indicates a huge peak between channels 360 and 370 which corresponds to the pedestal. This “pedestal peak” is broad and for that reason, the single photoelectron peak is not well separated from that peak and not quite visible. Also judged from the separation between the main peak and the hardly-visible single photoelectron peak, the pulse-height resolution obtained with the F1-ADC is slightly worse than that obtained with the traditional ADC.

3. ADC spectra of dE/dx counter

Figs. 6 (a) – (d) show the ADC spectra of the dE/dx counter obtained with F1-TDC-ADC at different thresholds. One can observe also here the “pedestal” peak at threshold 10 mV to 30 mV, but rather small. At 30 mV, the peak becomes very small, and at 40 mV, it almost disappears. Judged from these spectra, the threshold setting for dE/dx counter should be about 20 mV. The loss of small pulse-height events should be small at 20 mV. At 10 mV, the behavior of the ADC is slightly curious. One observes a double peak corresponding to the “pedestal”.

4. Beam profile observed with dE/dx counter

There are 4 planes in dE/dx counter. From upstream side, these are plane A (x1), C (y1), B (x2) and D (y2) (see Fig. 14 later shown). The triggered beam profile obtained with these planes at threshold 30 mV are shown in Fig. 7. The histograms shown from left to right, from top to bottom are, (a) the profile recorded by plane A, (b) the profile recorded by plane B, (c) the correlation of the hits between the plane A and B, (d) the profile recorded by plane C, (e) the profile

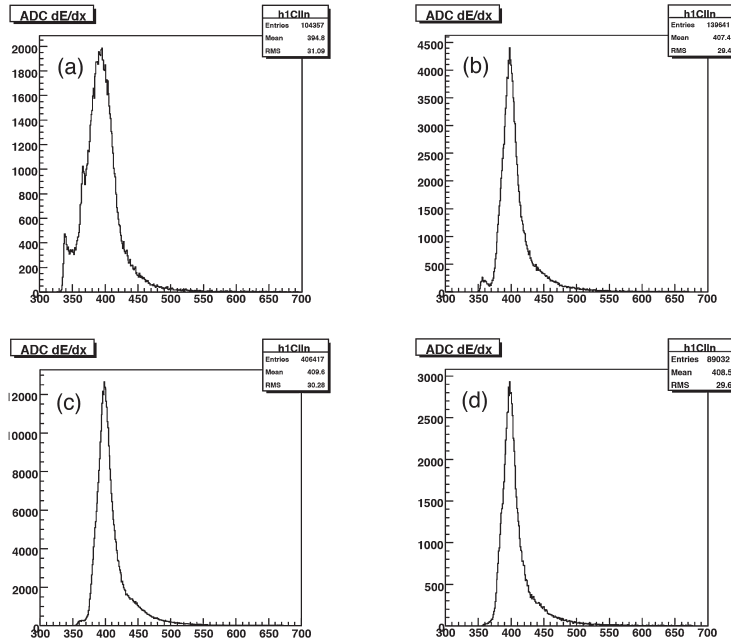


Fig. 6 ADC spectra obtained from dE/dx counter A plane with F1-ADC at different thresholds. Events included are those contained in the narrow timing peak shown in Fig. 2 (coincident events). The figures are for thresholds (a) 10 mV, (b) 20 mV, (c) 30 mV and (d) 40 mV.

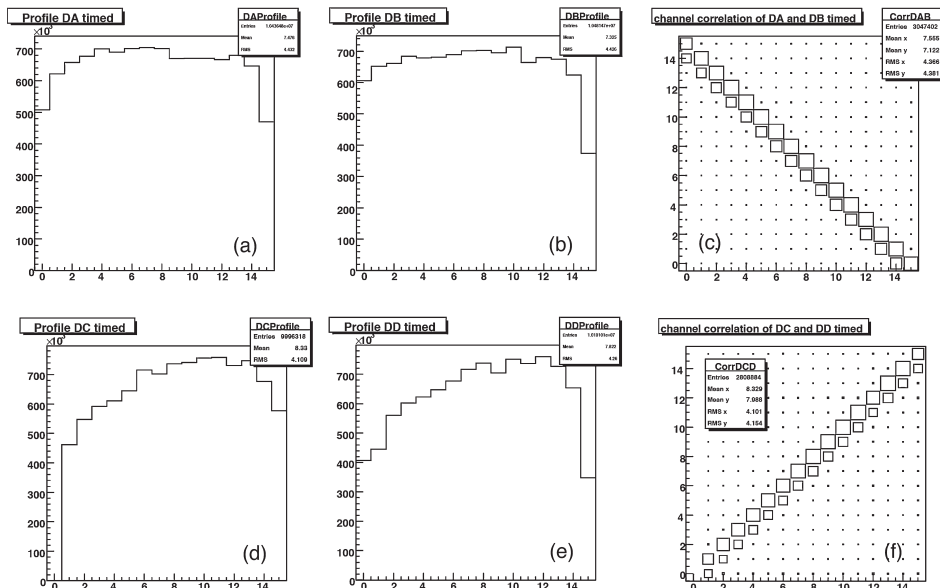


Fig. 7 Beam profile observed using A, B, C, D planes of dE/dx counter, and their correlations. The threshold set was 30 mV. The orientation of the planes is shown later in Fig. 14. Relatively smooth distribution is observed at this threshold.

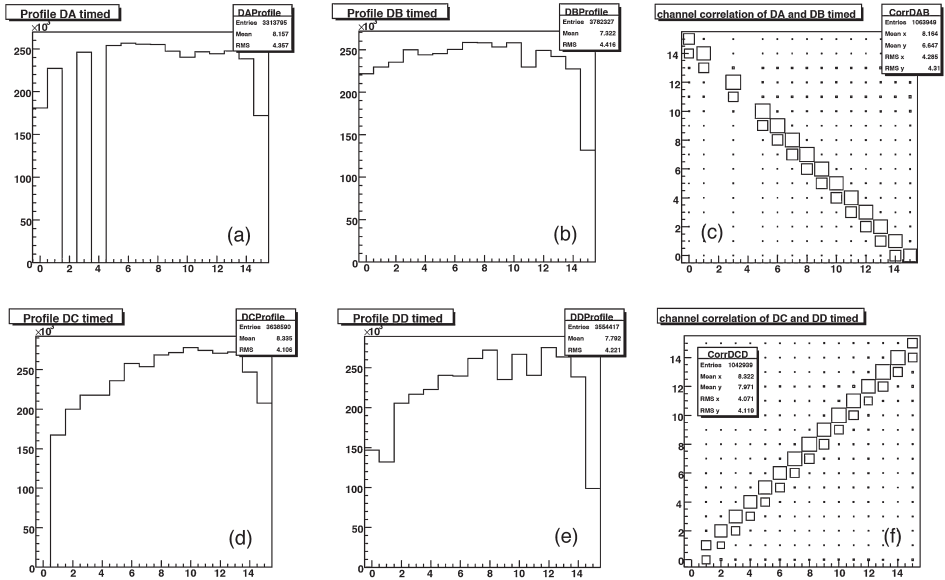


Fig. 8 Beam profile observed using A, B, C, D planes of dE/dx counter, and their correlations. The threshold set was 40 mV. The orientation of the planes is shown later in Fig. 14. The smooth distribution observed at 30 mV threshold is lost at this threshold

recorded by plane D, (c) the correlation of the hits between the plane C and D. The same histograms are shown in Fig. 8 for threshold 40 mV. It seems that at threshold 40 mV, one start losing the smoothness of the distribution observed at the threshold of 30 mV.

5. Beam Profile observed with X plane

Only 64 channels of X plane are read out in this measurement, and that corresponds to only 2/15 of the total plane. Nevertheless we show in Fig. 9 the beam profile observed with those 64 channels at different thresholds. It seems that at higher thresholds, the smoothness observed at 5 mV is lost. From this point of view, a threshold setting of 15 -20 mV seems to be most appropriate.

6. Multiplicity of the hits on X plane

Fig. 10 shows the multiplicity of the hits recorded by X plane. Here, multiplicity means just the number of hits found in a trigger. The left-side figure shows all the events included in the trigger, whereas the right-side figure shows only the events in the narrow peak in the TDC spectrum

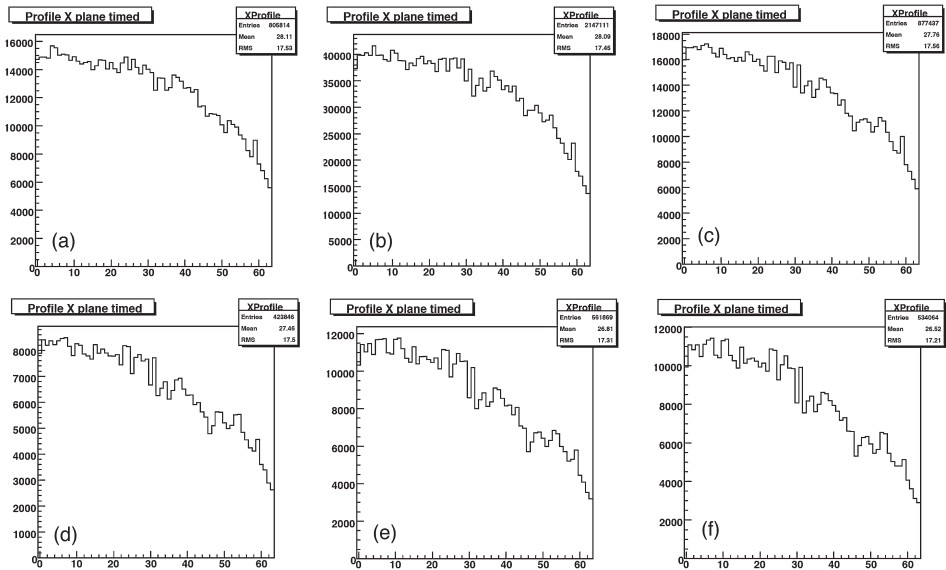


Fig. 9 Beam profile observed using X plane at different thresholds. The thresholds set are (a) 5 mV, (b) 10 mV, (c) 15 mV, (d) 20 mV, (e) 25 mV and (f) 30 mV. The smoothness of the distribution observed at 5 mV threshold starts to be lost at 20 mV.

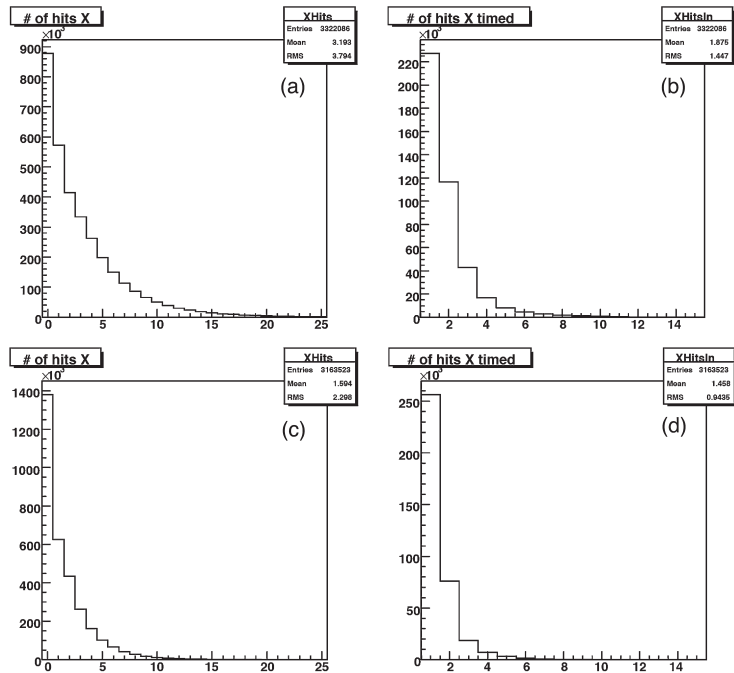


Fig. 10 Multiplicity of hits on X plane at threshold 5 mV (a and b) and 30 mV (c and d). The left histograms contain all the events included in the trigger, whereas in the right histograms contain only the events included in the narrow peak in Fig. 3 (coincident events). Note should be taken that these figures are only for the 2/15 of the total plane.

shown in Fig. 3 (coincident events). The figures above are for threshold 5 mV and the below are for 30 mV. Note should be taken that this is only for 2/15 of the X plane, and the multiplicity can be larger if the total plane is read out. For the left-side figures, one can comment that although the multiplicity is slightly reduced with the raised threshold, it is still very large, and this will increase the size of the data words. For the meaningful events in the right-side figures, the threshold dependence is not so large. The average multiplicity is about 2 at a reasonable threshold. However, again, this is only for 2/15 of the X plane, and it can be substantially larger for the whole X plane.

7. Multiplicity of the hits on dE/dx counter

Fig. 11 shows the multiplicity observed with the dE/dx counter (plane A). The top figures are for the threshold 10 mV, while the bottom figures are for 40 mV. The figures on the left side are for the total events included in the trigger, whereas the figures on the right side are for events included in the narrow peak in the TDC spectrum. It should be noted that the average multiplicity

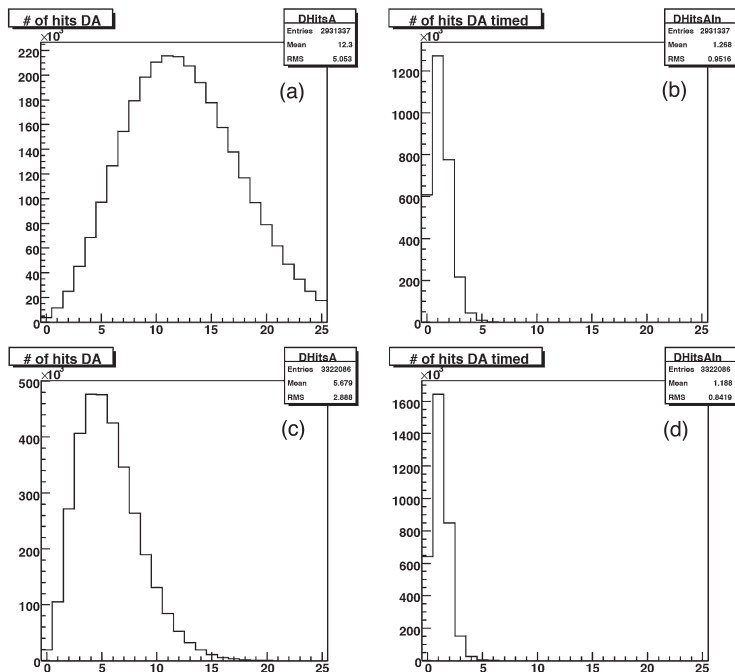


Fig. 11 Multiplicity of hits observed on the dE/dx counter plane A. At threshold 10 mV (a) the multiplicity of all the events in the trigger is as high as 12, whereas at 40 mV (c), it is reduced to 6 at 40 mV. However, the multiplicity of the hits in the narrow peak in Fig. 3 (coincident events) changes only slightly at different thresholds (b: 10mV, d: 40mV).

in the total events depend strongly on the threshold whereas the dependence is very small for the coincident events.

8. F1-TDC output and the time resolution

The time resolution of the X plane + F1-TDC system was calculated from the F1-TDC spectra. Column 8 of X plane was arbitrarily chosen, and the peak of its F1-TDC spectra obtained at different thresholds were fitted with a Gaussian. The result is shown in Fig. 12. To convert the number of channels of F1-TDC to ns, the designed conversion factor 120 ps/chan was used. The time resolution becomes better at higher thresholds, but still is much worse than the resolution of 600 ps obtained with the LeCroy 3377 TDC. One of the main reasons is that in this test, the time resolution of the trigger signal is not guaranteed to be good. Also this trigger contains fast and slow particles. If one wants to find the real time resolution, one has to put a window on the speed and kind of the particles.

The same exercise was performed for the A plane of dE/dx counter. The result is shown in Fig. 13. Also first slab among 16 of A plane was chosen arbitrarily. By virtue of the larger light output than in X plane, the apparent time resolution is slightly better than with X plane. However, we do not consider this resolution to be the real one for the reason indicated above. In this display also, a conversion factor of 120 ps/chan was used.

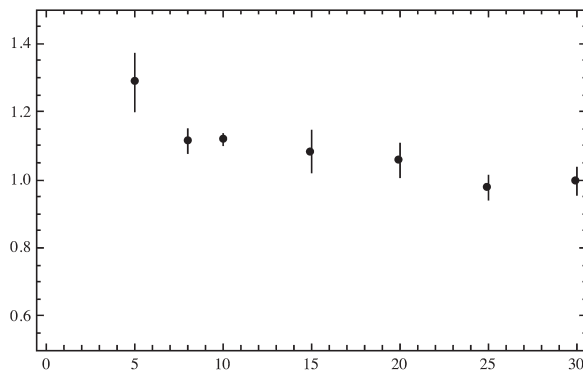


Fig. 12 Time resolution of X plane read out using F1-TDC from the timing peak of column 8 (unit ns) dependent on the threshold set (horizontal axis, unit: mV). The conversion from the F1-TDC output to the timing was done using 120 ps/chan, the designed conversion factor. The absolute value of the timing resolution observed is worse than in case the plane was read out using PSC and LeCroy 3377 TDC. However, we believe that this is not the real time resolution of the system for the reasons explained in the text.

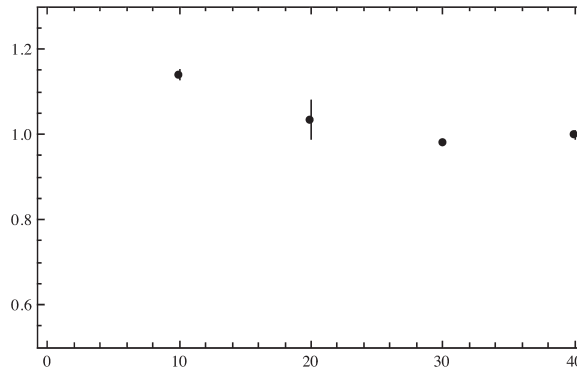


Fig. 13 Time resolution of dE/dx counter plane A read out using F1-TDC from the timing peak of slab 0 (unit ns) dependent on the threshold set (horizontal axis, unit: mV). The conversion from the F1-TDC output to the timing was done using 120 ps/chan, the designed conversion factor. There is a possibility that the time resolution thus estimated is much worse than the reality.

9. Efficiency of X plane

The number of the read-out columns of X plane is only 64, and its coverage of the dE/dx counter slabs is hardly perfect. Nevertheless, we try to evaluate the efficiency of X plane, not quite the absolute value, but rather the threshold dependence of the efficiency. For that purpose, we select events with the 1st slab of dE/dx plane A (x1) and all the slabs of the 2nd plane B (y1) excluding the 2 slabs at the edges in coincidence. This event selection is schematically shown in Fig. 14.

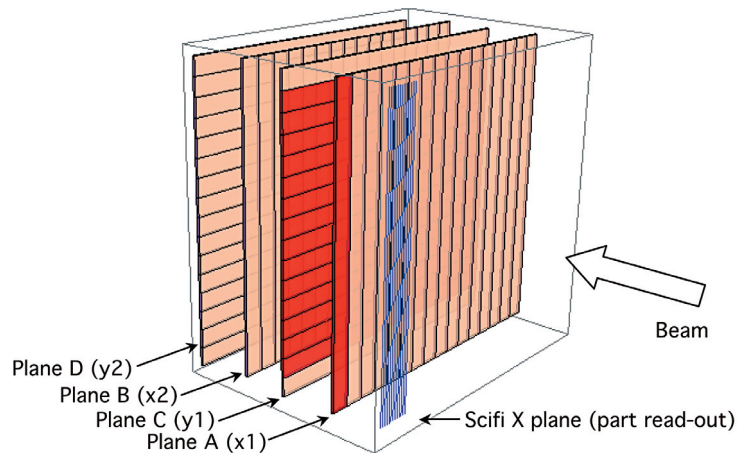


Fig. 14 The configuration of X plane, and the planes A, B, C, D of dE/dx counter. Out of 480 channels of X plane, only 64 channels were read out with F1-TDC-ADC. This figure shows also how the event selection was made to evaluate the efficiency of X plane. Slab 0 of plane A, slab 1 to 14 of the C plane were used for the event selection.

Table Offsets of the planes of dE/dx counter

plane	name	slabs	direction	amount
A	x1	16	x	0
C	y1	16	y	0.6 mm
B	x2	16	x	-2.56 mm
D	y2	16	y	-1.56 mm

The results are shown in Fig. 15 in the case of threshold for X plane (threshX) 15 mV and threshold for dE/dx counter (threshD) 40 mV.

Fig. 15 (a) and (b) show the correlation between the X plane columns (horizontal axis) and the A (x1) plane slabs (vertical axis), and also with B plane (y1) slabs (vertical). The multiplicity of the X-plane hits of the events thus selected is shown in (c). In this event selection we require single hits on dE/dx A plane and also on C plane. Thus it is rather surprising that there are fairly many events with multiplicity larger than 1. If we consider the alignment to be perfect, this means that in the events recorded by dE/dx counter, there are non-negligible double hits. (We will come back to this point later.) For those selected events, their profile on X plane is shown in (d). The coverage of the slab 0 of plane A of the 64 columns of X plane seems not so bad judging from the histogram. But to evaluate the efficiency at the level of 1/10 of percent, we see that it is not per-

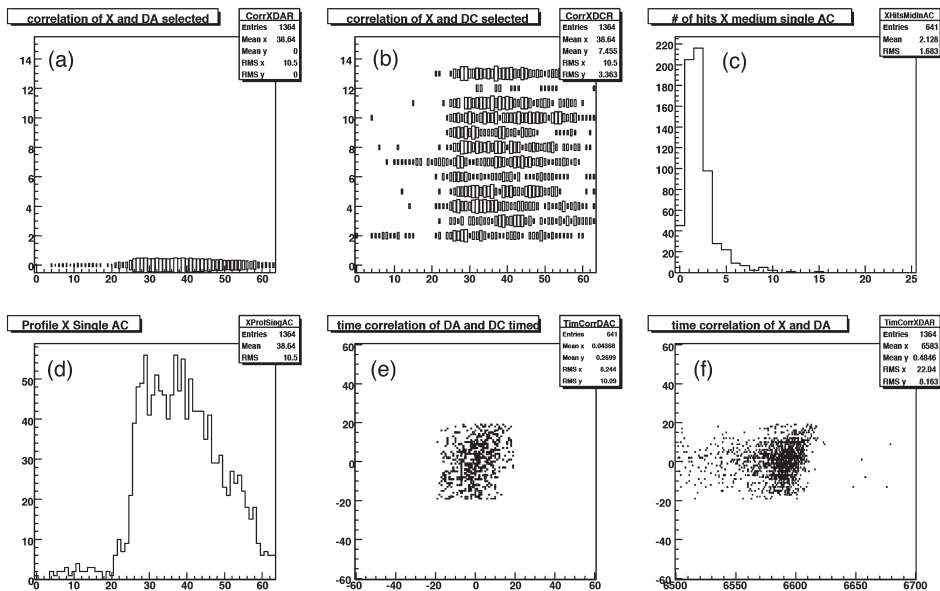


Fig. 15 The result of the event selection performed for the evaluation of the efficiency of X plane. The figures shown are, from left to right, top to bottom, (a) the correlation of hits between X plane columns (horizontal) and the slabs of plane A of dE/dx counter (vertical), (b) the correlation of hits between X plane columns and (horizontal) and plane C of dE/dx counter, (c) multiplicity of the hits on X plane, (d) profile (histogram) of the X-plane columns, (e) timing of the selected hits, horizontal: A plane, vertical: C plane, and (f) timing of the selected events, horizontal: X plane, vertical: A plane.

fect. In this evaluation of the efficiency, we select single hit on both plane A and B with a rather tight cut (± 2.4 ns) in timing, as shown in the vertical axes of Fig. 15 (e) and (f) respectively, whereas the time window applied to the X-plane hits are a little wider (± 50 TDC channels which means 6.25 ns.) The efficiency namely the number of events recorded hits on X plane among those events selected by dE/dx planes is 93.3 % at threshX = 5 mV. It is obvious from Figs (a) and (d) that the coverage of the X plane is not perfect.

We carried out the same exercise with plane A+D (y_2) of dE/dx counter as shown in Fig. 16 (a), and also with plane C (x_2) + B counters as shown in Fig. 16 (b).

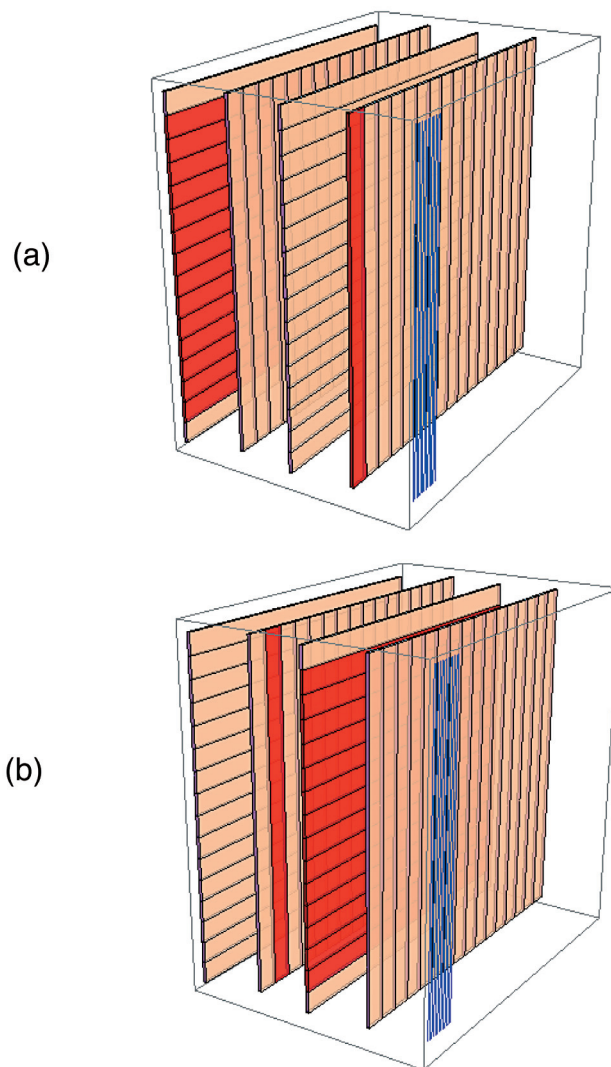


Fig. 16 (a) event selection using A and D (y_2) planes. (b) event selection using B (x_2) and C planes.

The results of the measurements with the same thresholds are shown in Figs 17 and 18.

The efficiencies are calculated as 93.5% and 90.9%, respectively. Now, Fig. 19 shows the dependence on the X-plane threshold of the efficiency for different event selections.

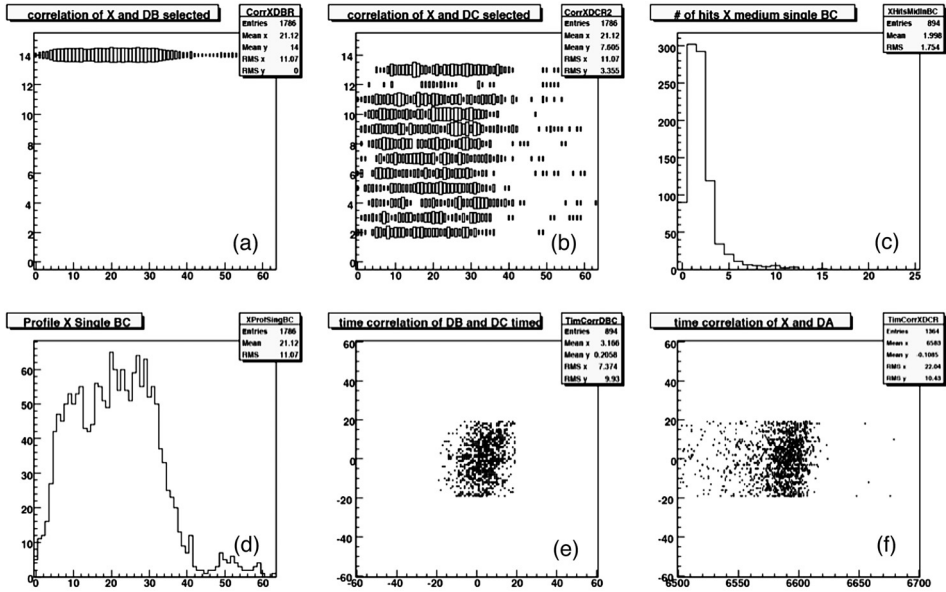


Fig. 17 The result of the event selection performed for the evaluation of the efficiency of X plane. For the explanation of figures, see Fig. 15. Planes A and D (yz) were used for the event selection.

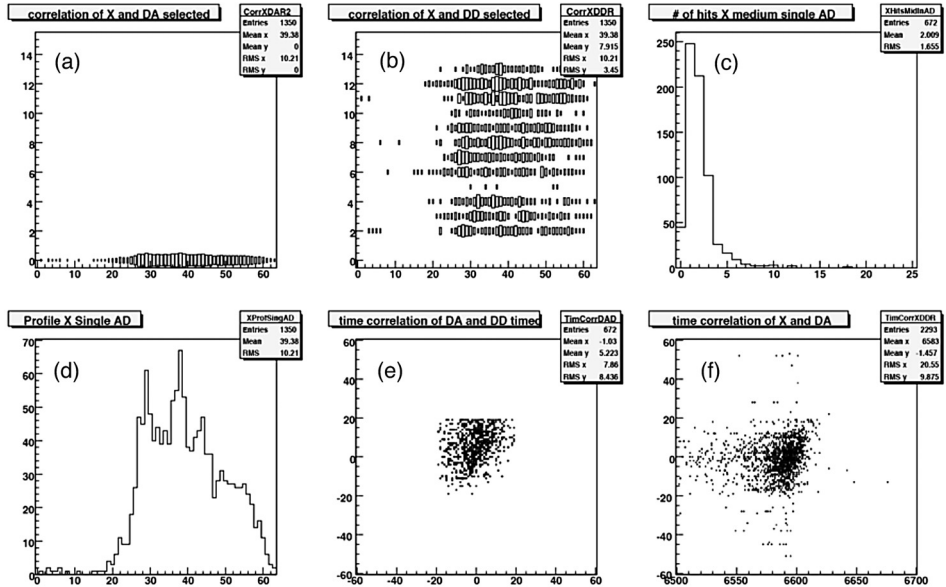


Fig. 18 The result of the event selection performed for the evaluation of the efficiency of X plane. For the explanation of figures, see Fig. 15. Planes B(x2) and C were used for the event selection.

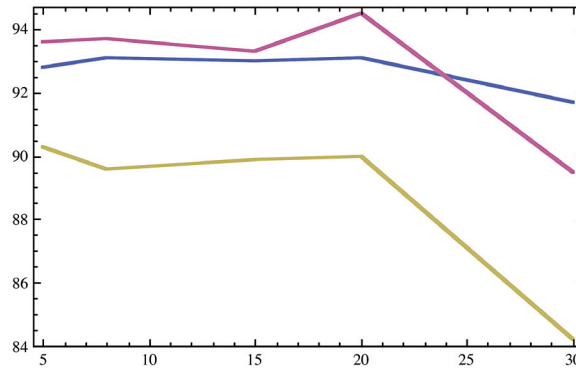


Fig. 19 The evaluation of the efficiency of X plane performed as explained. As already explained above, we cannot extract the absolute value of the efficiency. We should pay more attention to the threshold dependence of the efficiency. Up to threshold of 15 mV, the efficiency is rather constant, but above 20 mV, we start losing.

From this figure, we probably can tell that up the 15 mV, we do not lose efficiency. But the absolute value which is at most 94% from this figure is not meaningful, as we said before that the coverage is not good enough. For the absolute value of the efficiency, we need to have an integral DAQ which allows us to make a projection of the tracks starting from the backward counters.

10. ADC information of the dE/dx counter - once again

It is interesting that we observe fairly many events which register multiple hits on the X plane in the exercise in the preceding chapter, as shown in Figs 15 (c), 17 (c) and 18 (c) although we require single hits on the dE/dx slabs. Those are events which look single on dE/dx counters, but fire multiple columns on X plane, that means events which look like atomic pairs. It is thus very interesting to analyze the ADC output of those events on the dE/dx planes. It might allow to check the real performance of the F1-ADC in distinguishing single and double hits.

Fig. 20 shows events collected with $\text{threshX} = 15$ mV and $\text{threshD} = 40$ mV. Upper row from left to right show (a) correlation between the F1-ADC output and the multiplicity on X plane, (b) ADC spectrum of the X-plane single-hit events, and (c) ADC spectrum of the multiple-hit events. Events were selected with slab 0 of dE/dx A plane and slab 1 through 14 of C plane. Then the lower row shows the same histograms but with events selected with slab 14 of the B plane and slab 1 through 14 of the D plane. It seems rather obvious that we see peaks corresponding to single and double charge in the ADC spectra. It is surprising that these peaks are so well seen despite the fact that Landau tail can fairly easily wipe out these structures.

To be sure that this phenomenon is not only a play of the statistics, we will show another case

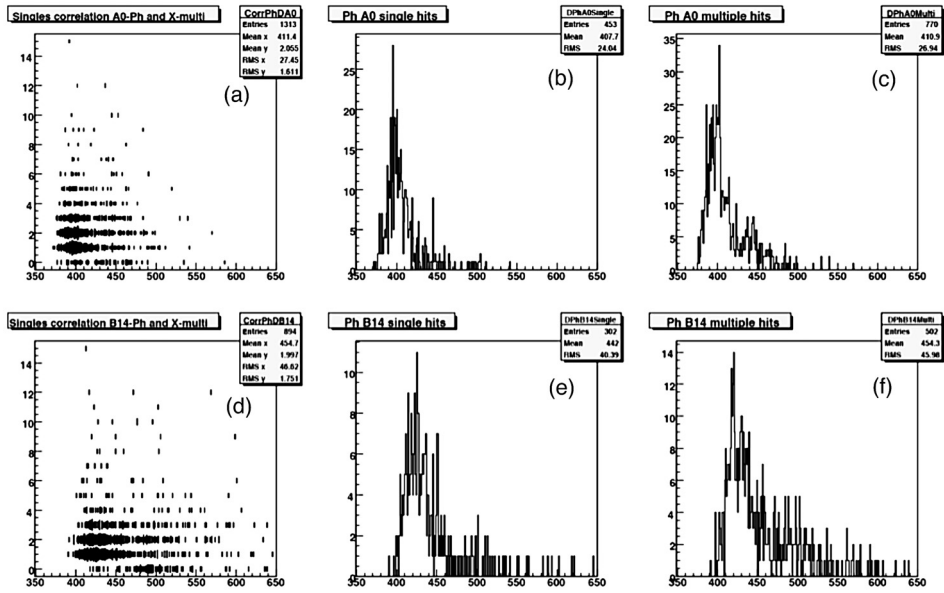


Fig. 20 (a and d): Correlation of the multiplicity of X plane of the events selected in Chap. 9 (horizontal axis) and the F1-ADC spectrum of dE/dx counter A plane. (b and e): ADC spectrum for single-hit events, (c and f): double and more than double-hit events. Top row (a,b,c) is with event selection with dE/dx counter plane A and C. Bottom row (d,e,f) is with plane B and C. The thresholds were: threshX = 15 mV and threshD = 40 mV.

in Fig. 21 where the histograms are the same, but the events were collected with threshX = 10 mV and threshD = 30 mV.

One can clearly see the trend, and also the ADC gain which is higher in strip 14 of plane B than strip 0 of plane A can be confirmed.

11. Profile scan of X plane

The mini-DAQ used allows only 128 channels to register at a time. There are in total 480 columns in X plane, and Sosuke took 4 shots to scan the full surface of X plane. Fig. 22 through 25 show the profile of the scan of X plane thus obtained.

The top figures show the profile with all the hits registered within the full time window, whereas the bottom figures contain only hits on the X plane within a narrow time window of 50 TDC channels (~ 6 ns). In this case also, if the multiplicity of the X-plane hit is more than 1, all the hits are included in the figures. One can notice that 2 channels are missing, but this is due to a bad contact of the connectors which can be easily fixed. The data have been taken with a hardware threshold threshX at 10 mV.

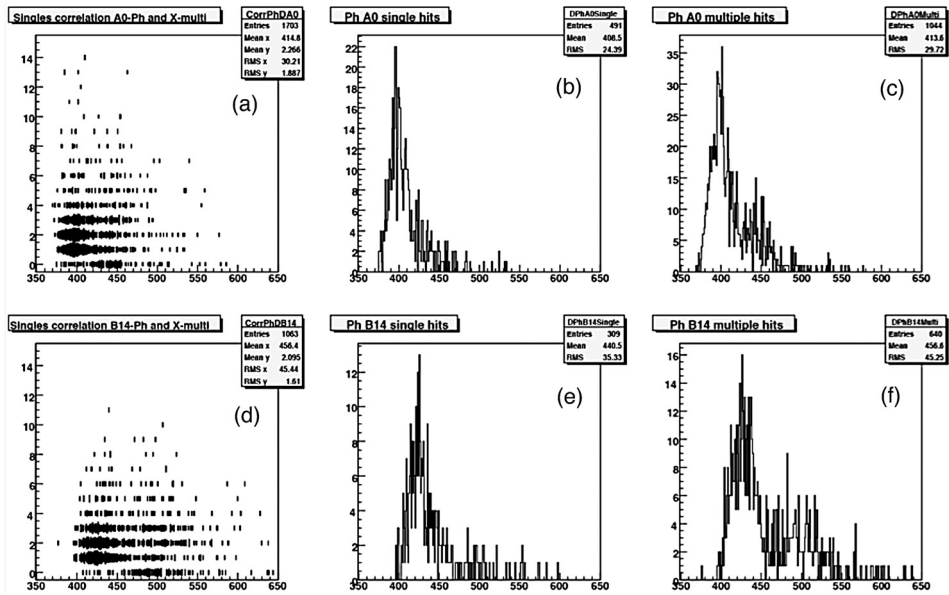


Fig. 21 (a and d): Correlation of the multiplicity of X plane of the events selected in Chap. 9 (horizontal axis) and the F1-ADC spectrum of dE/dx counter A plane. (b and e): ADC spectrum for single-hit events, (c and f): double and more than double-hit events. Top row (a,b,c) is with event selection with dE/dx counter plane A and C. Bottom row (d,e,f) is with plane B and C. The thresholds were: threshX = 10 mV and threshD = 30 mV.

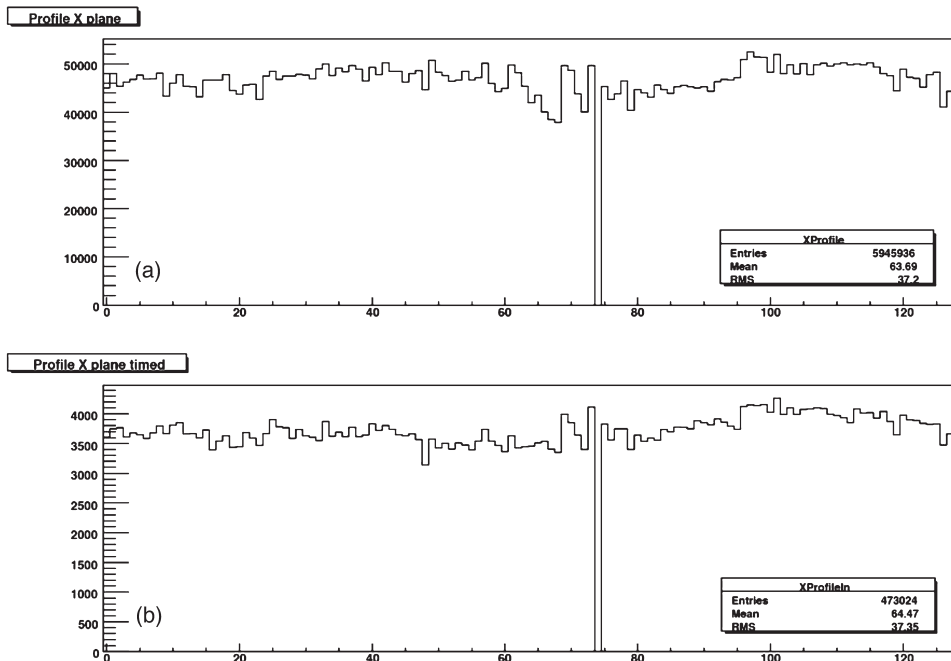


Fig. 22 Profile recorded by X plane read out with F1-TDC-ADC. The X plane channels covered are chan. 64 – 191. (a) All trigger events, (b) coincident events only.

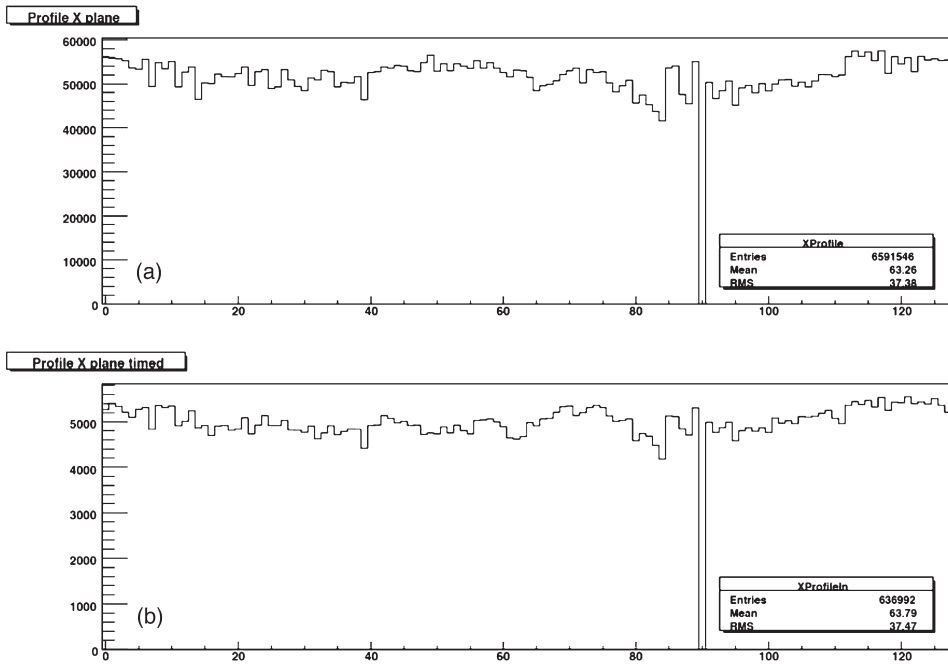


Fig. 23 Profile recorded by X plane. The covered are chan. 80 - 207.

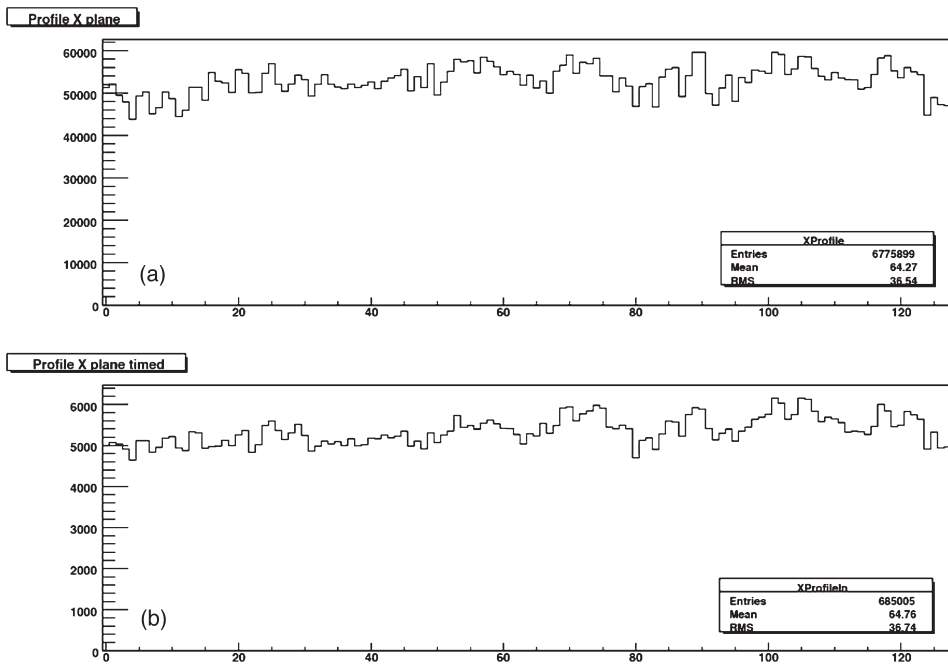


Fig. 24 Profile recorded by X plane. The covered are chan. 208 - 335.

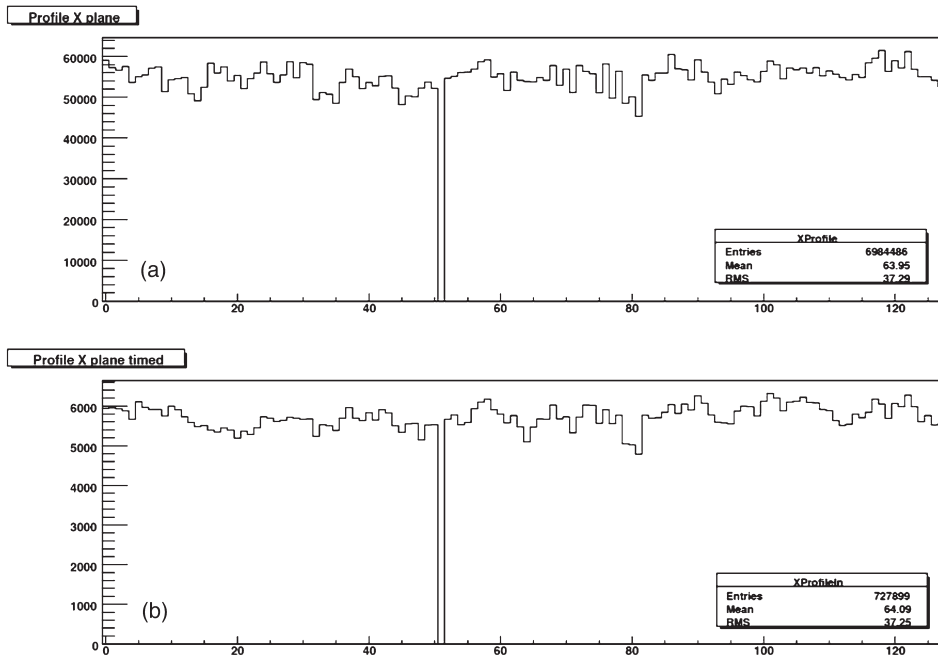


Fig. 25 Profile recorded by X plane. The covered are chan. 336 - 463.

One can notice a very flat profile which guarantees 1) The uniformity of the fiber bundle construction, and 2) The uniform threshold setting of the F1-TDC device.

12. Conclusion

The main objective of this analysis was to check the performance of the F1-TDC-ADC device, and to find the most appropriate threshold for X plane (and for dE/dx counter).

As TDC device, it seems that the threshold setting is reproducible. This is very important for a long-term measurement such as DIRAC experiment. The TDC spectra obtained are reasonable, but the time resolution extracted from its TDC spectra was not as good as before. But the main reason for that is not due to the performance of the device, and it must be rather due to the measurement conditions. As an ADC device, it can reproduce the spectra that we used to see with LeCroy 2228A ADC, although the resolution of the F1 device seems not as good as that of the traditional ADC. The most important problem is the “pedestal” peak which appears where one expects to see the pedestal. The pedestal which is caused by the zero level of the signal within the gate in the traditional ADC is contained in only one or two channels, whereas with F1 device,

it is much broader. The observation of the single photoelectron peak which our PSPM H6568MOD allows (very special feature of this PM) becomes difficult. Thus in conclusion, if the amount of light is larger and the dynamic range is small, as in the case of dE/dx counter, this device gives a huge advantage since it allow to observe ADC information of each of the multihit events. As shown in Chap. 10, this ADC seems to separate fairly well the single and double peak on dE/dx counter. If this feature is really confirmed with data with more appropriate DAQ, it must be a very good news for DIRAC experiment.

As for the setting of the threshold, the most appropriate threshold of X plane is 15 - 20 mV. This is judged from the beam profile shown in Fig. 9, time resolution shown in Fig. 12, efficiency curve shown in Fig. 19, and the ADC spectrum shown in Fig. 4. For dE/dx counter, the most appropriate threshold seems to be 20 mV. From the timing resolution, the threshold of 20-30 mV is acceptable, and the beam profile for 30 mV shown in Fig. 7 seems still acceptable. However, in the ADC spectrum shown in Fig. 6, it might be that we start losing very small signals already at 30 mV.

As for the performance of X plane, the result from the data analysis of the scanned data shown in Chap. 11 is very encouraging. The event rate is very uniform. There are a few missing channels, but those are probably due to some bad contact at the level of connectors, and can be fixed from our past experience.

Before, with the PSC and LeCroy 3377 read out, the adjustment of the threshold, channel by channel of Scifi plane was very difficult. Now, it is rather easy to adjust the threshold with F1-TDC-ADC device at the firmware level. Of course, it is now possible to adjust them in the off-line analysis too, as we have the pulse-height information of each hit.

References

- [1] High resolution scintillating-fibre hodoscope and its readout using Peak-sensing algorithm, A. Gorin et al., Nucl. Instr. Meth. in Phys. Res. A **566** (2006) 500-515
- [2] First measurement of the $\pi^+\pi^-$ atom lifetime, B. Adeva et al. ,Phys. Letters B 619 (2005) 50-60;
Detection of $\pi^+\pi^-$ atoms with the DIRAC spectrometer at CERN, B. Adeva et al., Journal of Physics G **30** (2004) 1929-1946;
DIRAC: A high resolution spectrometer for ponium detection, B. Adeva et al., Nucl. Inst. Meth. in Phys. Res. **A515** (2003) 467-496;
The multilevel trigger system of the dirac experiment, L. Afanasyev et al., Nucl.Instrum.Meth.**A491** (2002) 376-389
- [3] Peak-sensing discriminator for multichannel detectors with cross-talk, A. Gorin et al., Nucl. Instr. Meth. in Phys. Res. **A452** (2000) 280-288

- [4] Test and tuning of the newSFD detectors at T11 beam line, F. Takeuchi et al., Bulletin of the research institute of advanced technology **5** (2007) 57-76